ORIGINAL PAPER

Theoretical studies on the structure, thermochemical and detonation properties of amino and nitroso substituted 1,2,4-triazol-5-one-N-oxides

P. Ravi · V. Venkatesan · Surya P. Tewari

Abstract DFT calculations at the B3LYP/aug-cc-pVDZ level have been carried out to explore the structure, stability, electron density, heat of formation, detonation velocity and detonation pressure of substituted amino- and nitroso-1,2,4-triazol-5-one-N-oxides. Heats of formation of substituted triazol-5-one-N-oxides have been computed at the B3LYP/aug-cc-pVDZ level via isodesmic reaction procedure. Materials Studio 4.1 package was used to predict the crystal density of model compounds. Kamlet-Jacob equations were used to calculate detonation properties based on the calculated heat of explosion and crystal density. The designed compounds **4**, **6**, **7** and **8** have shown higher performance compared with those of 2,4,6,8,10,12-hexanitro-2,4,6,8,10,12-hexaazaisowurtzitane and octanitro-cubane. Atoms-in-molecule (AIM) analyses have also been carried out to understand the nature of intramolecular interactions in the designed molecules.

Keywords Crystal density · Detonation pressure · Detonation velocity · DFT method · Electron density · Heats of formation

Introduction

Nitrotriazoles have drawn renewed attention due to their positive heat of formation, high nitrogen content, good thermal stability and favorable detonation performance [1]. The exceptional stability of 3-nitro-1,2,4-triazol-5-one is due to the high degree of hydrogen bonding carbonyl and nitro groups along with the molecular symmetry which allows the molecule to

P. Ravi (✉) · S. P. Tewari
Advanced Centre of Research in High Energy Materials,
University of Hyderabad, Hyderabad 500 046, India
e-mail: rpiitb@hotmail.com

V. Venkatesan
High Energy Materials Research Laboratory, Sutarwadi,
Pune 411021, India

form the layered crystal structure [2]. Thermochemical and molecular properties such as heats of formation and crystal density are the important parameters to determine the explosive properties of materials. To calculate the detonation velocity and detonation pressure, we require the heat of detonation, number of decomposition products and their average molecular weight and density of energetic compounds.

The presence of nitro (NO_2), nitroso (N=O) group, N-oxide (N→O) and carbonyl (C=O) bonds in the N-heterocycles increases the heat of formation, density and thus detonation velocity and detonation pressure [3]. Also the introduction of amino (NH_2) group(s) into azoles decreases the sensitivity of the product relative to the unaminated starting materials. The present study aims to aid in the design of 1,2,4-triazol-5-one-N-oxides for explosives applications by uncovering the structure–property relationships. The density functional theory calculations at the B3LYP/aug-cc-pVDZ level were carried out to study the geometric and electronic structures, thermodynamic properties and detonation properties of triazol-5-one-N-oxides. We also have addressed how the relative positions of amino, nitroso, carbonyl and N-oxide groups (i.e., the relative positions of N-atoms in the ring) affects the heat release, density and detonation velocity and pressure of triazolone-N-oxides.

Computational details

Optimized geometries for the triazol-5-one-N-oxides were calculated at the B3LYP/aug-cc-pVDZ level of theory using Gaussian 03 package [4]. This B3LYP density functional theory method combines the three-parameter Becke exchange functional (B3) with the Lee−Yang−Parr (LYP) correlation functional [5–9]. After the geometry of each structure had been optimized and the energies obtained, frequency calculations were performed at the same level of theory to confirm that the structures obtained were minima on the potential

energy surface. This level of theory has been shown to be adequate for obtaining fairly accurate geometries, vibrational frequencies, and zero point energies [10].

Isodesmic reaction methodologies have been followed to calculate the heats of formation of triazol-5-one-N-oxides. Isodesmic reaction is a hypothetical chemical process in which the number of bonds of each formal type remains the same on each side of the equation but with changes occurring in their mutual relationships. This method has been found to yield satisfactory results [11]. To minimize errors during the calculations, triazoles (1,2,3-triazole and 1,2,4-triazole) were kept intact and taken as one of the reference compounds. Scheme 1 & 2 represents the general isodesmic reactions to estimate the heats of formation of title compounds.

The heat of reaction $\Delta_f H^0$ at 298 K can be calculated through reaction enthalpies:

$$\Delta H_{298.15 \text{ K}} = \sum_{\text{Products}} \Delta_f H^0 - \sum_{\text{Reactants}} \Delta_f H^0 \qquad (1)$$

where $\sum_{\text{Products}} \Delta_f H^0$ and $\sum_{\text{Reactants}} \Delta_f H^0$ are sum of the heats of formation for products and reactants in gas at 298.15 K respectively. Since the experimental heats of formation of reference compounds (CH_4, CH_3NH_2, CH_3ONO_2, 1,2,3-triazole and 1,2,4-triazole) are available [12], the heats of formation of triazol-5-one-N-oxides can be obtained if the heats of reaction are known. The heat of explosion (Q) can be calculated from the difference between sum of the energies for the formation of explosive components and sum of the energies for the formation explosive products.

$$Q = \Delta E_{298 \text{ K}} + \Delta(PV) = \Delta E_0 + \Delta ZPE + \Delta_T H \\ + \Delta nRT \qquad (2)$$

where ΔE_0 is the change in total energy between the products and reactants at 0 K; ΔZPE is the difference between the zero point energies of the products and reactants; $\Delta_T H$ is the difference between the thermal correction from 0 to 298.15 K of the products and reactants; $\Delta(PV)$ equals to ΔnRT. $\Delta n=0$ for an ideal gases.

The optimized structures have been used to determine the densities of triazol-5-one-N-oxides using Materials Studio 4.1 package with cvff, dreiding, universal, compass, compass26 and compass27 force fields [13]. Poltizer et al. [15] approach also was followed to estimate the crystal density by the following expression:

$$\rho = \alpha_1 \left(\frac{M}{V_m} \right) + \beta_1 \left(v\sigma_{\text{tot}}^2 \right) + \gamma_1 \qquad (3)$$

where M is the molecular mass (g/molecule) and V(0.001) is the volume (cm^3/molecule) defined as the space inside as contour of electron density of 0.001 electron/$Bohr^3$. α, β and γ are regression coefficients. v is the degree of balance between the positive and negative charges on the isosurface. σ_{tot}^2 is a measure of variability of the electrostatic potential on the surface.

Kamlet-Jacob equations [15] were used to determine the detonation velocity and detonation pressure:

$$D = 1.01 \left(NM^{1/2}Q^{1/2} \right)^{1/2} (1 + 1.30 \ \rho) \qquad (4)$$

$$P = 1.558 \ NM^{1/2}Q^{1/2}\rho^2 \qquad (5)$$

where D is the detonation velocity in km/s, P is the detonation pressure in GPa, N is the number moles of gaseous detonation products per gram of explosive, M is the average molecular weight of gaseous products, Q is the energy of explosion in cal/g of explosive and ρ is the density in g/cm^3.

The possible detonation products of triazol-5-one-N-oxides have been written based on the modified Kistiakowsky-Wilson rules [16]:

$$C_2H_3N_5O_3 \rightarrow 1½ \ H_2O + 1½ \ CO + ½ \ C + 2½ \ N_2 \qquad (6)$$
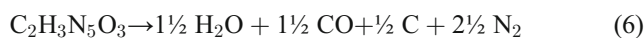
The highest occupied molecular orbitals and the lowest unoccupied molecular orbitals are known to play a key role in governing the chemical reactions. The band gap between the frontier molecular orbital energies is an important stability index of the molecules [17, 18]. We have calculated the stability of 1,2,4-triazol-5-one-N-oxides from the total energy, frontier molecular orbital energies and their gaps.

The strength of bonding can be evaluated by the bond dissociation energy. The energy required for homolytic bond cleavage at 298 K and 1 atm corresponds to the enthalpy of

Scheme 1 Isodesmic reaction used for the estimation of heat of formation of 1,2,4-triazol-5-one-N-oxides

where X, Y, Z = NH_2, NO, H
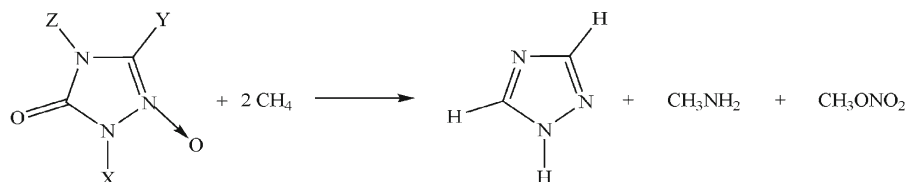
Scheme 2 Isodesmic reaction used for the estimation of heat of formation of 1,2,3-triazol-5-one-N-oxides

where X, Y, Z = NH_2, NO, H
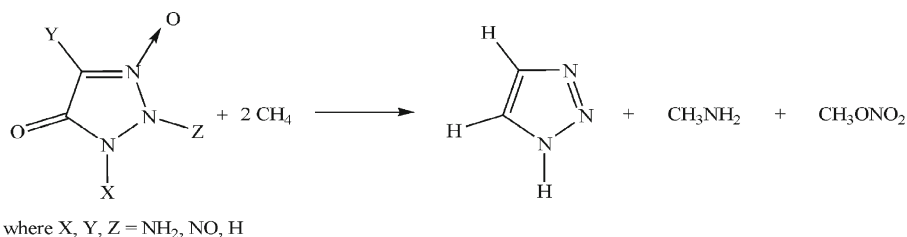
Fig. 1 Optimized structures of model molecules at the B3LYP/aug-cc-pVDZ level. The arrow indicates the weakest bond based on electron density analysis
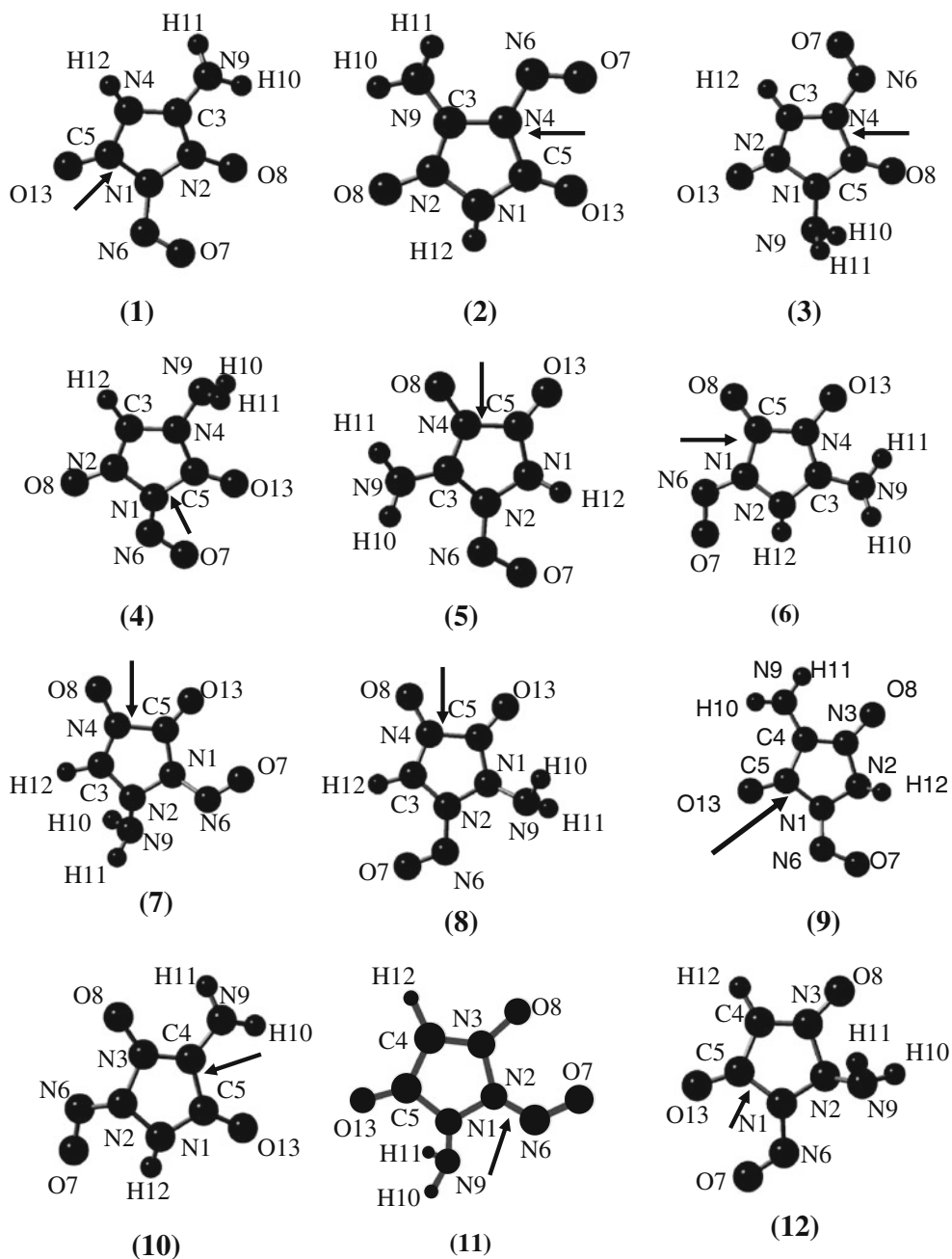
**Table 1** Selected structural parameters[a] of triazol-5-one-N-oxides computed at the B3LYP/aug-cc-pVDZ level

Parameter	1	Parameter	2	Parameter	3	Parameter	4	Parameter	5	Parameter	6
N1-N2	1.457	N1-N2	1.426	N1-N2	1.468	N1-N2	1.448	N1-N2	1.396	N1-N2	1.408
N2-C3	1.316	N2-C3	1.31	N2-C3	1.316	N2-C3	1.314	N2-C3	1.378	N2-C3	1.387
C3-N4	1.384	C3-N4	1.393	C3-N4	1.395	C3-N4	1.387	C3-N4	1.332	C3-N4	1.335
N4-C5	1.394	N4-C5	1.448	N4-C5	1.420	N4-C5	1.386	N4-C5	1.449	N4-C5	1.426
C5-N1	1.425	C5-N1	1.387	C5-N1	1.392	C5-N1	1.430	C5-N1	1.412	C5-N1	1.437
N1-N6	1.426	N4-N6	1.399	N4-N6	1.382	N1-N6	1.437	N2-N6	1.345	N1-N6	1.347
N6-O7	1.188	N6-O7	1.200	N6-O7	1.210	N6-O7	1.188	N6-O7	1.223	N6-O7	1.219
N2-O8	1.277	N2-O8	1.274	N2-O8	1.236	N2-O8	1.253	N4-O8	1.288	N4-O8	1.297
C3-N9	1.367	C3-N9	1.363	N1-N9	1.365	N4-N9	1.395	C3-N9	1.338	C3-N9	1.337
N9-H10	1.015	N9-H10	1.012	N9-H10	1.017	N9-H10	1.021	N9-H10	1.009	N9-H10	1.009
N9-H11	1.018	N9-H11	1.015	N9-H11	1.015	N9-H11	1.019	N9-H11	1.015	N9-H11	1.019
N4-H12	1.011	N1-H12	1.015	C3-H12	1.079	C3-H12	1.079	N1-H12	1.017	N2-H12	1.022
C5-O13	1.205	C5-O13	1.203	C5-O13	1.206	C5-O13	1.209	C5-O13	1.197	C5-O13	1.195
N1-N2-C3	106.4	N1-N2-C3	108.3	N1-N2-C3	107.1	N1-N2-C3	106.4	N1-N2-C3	108.6	N1-N2-C3	103.3
N2-C3-N4	110.5	N2-C3-N4	108.9	N2-C3-N4	108.8	N2-C3-N4	110.0	N2-C3-N4	109.2	N2-C3-N4	112.6
C3-N4-C5	110.6	C3-N4-C5	109.4	C3-N4-C5	111.0	C3-N4-C5	111.4	C3-N4-C5	109.2	C3-N4-C5	109.7
N4-C5-N1	103.7	N4-C5-N1	102.7	N4-C5-N1	103.1	N4-C5-N1	102.7	N4-C5-N1	104.7	N4-C5-N1	102.5
C5-N1-N2	108.5	C5-N1-N2	109.9	C5-N1-N2	109.2	C5-N1-N2	109.2	C5-N1-N2	107.4	C5-N1-N2	115.5
H10-N9-H11	113.2	H10-N9-H11	115.8	H10-N9-H11	113.3	H10-N9-H11	107.6	H10-N9-H11	120.7	H10-N9-H11	120.1
N1-N6-O7	115.5	N4-N6-O7	115.3	N4-N6-O7	112.6	N1-N6-O7	113.2	N2-N6-O7	113.6	N1-N6-O7	113.2
O7-N6-N1-N2	−11.6	O7-N6-N4-C3	179.5	O7-N6-N4-C3	1.1	O7-N6-N1-N2	174.5	O7-N6-N2-N1	2.36	O7-N6-N1-N2	1.6
H10-N9-C3-N4	−171.6	H10-N9-C3-N4	−168.7	H10-N9-N1-N2	−120.2	H10-N9-N4-C5	−60.8	H10-N9-C3-N4	−165.9	H10-N9-C3-N4	159.6
H12-N4-C5-O13	14.0	H12-N1-C5-O13	−32.7	H12-C3-N4-C5	179.8	H12-C3-N4-C5	178.5	H12-N1-C5-O13	38.6	H12-N2-C3-N4	129.8
O8-N2-C3-N4	170.4	O8-N2-C3-N4	−178.9	O8-N2-C3-N4	−179.1	O8-N2-C3-N4	178.7	O8-N4-C5-N2	−174.5	O8-N4-C5-N1	−177.8

Parameter	7	Parameter	8	Parameter	9	Parameter	10	Parameter	11	Parameter	12
N1-N2	1.417	N1-N2	1.405	N1-N2	1.411	N1-N2	1.395	N1-N2	1.384	N1-N2	1.416
N2-C3	1.398	N2-C3	1.379	N2-N3	1.438	N2-N3	1.449	N2-N3	1.432	N2-N3	1.476
C3-N4	1.319	C3-N4	1.327	N3-C4	1.325	N3-C4	1.324	N3-C4	1.332	N3-C4	1.318
N4-C5	1.488	N4-C5	1.482	C4-C5	1.454	C4-C5	1.463	C4-C5	1.447	C4-C5	1.451
C5-N1	1.407	C5-N1	1.389	C5-N1	1.431	C5-N1	1.406	C5-N1	1.415	C5-N1	1.448
N1-N6	1.453	N2-N6	1.382	N1-N6	1.354	N2-N6	1.379	N2-N6	1.761	N1-N6	1.465
N6-O7	1.184	N6-O7	1.212	N6-O7	1.217	N6-O7	1.213	N6-O7	1.142	N6-O7	1.183
N4-O8	1.262	N4-O8	1.258	N3-O8	1.254	N3-O8	1.251	N3-O8	1.242	N3-O8	1.232
N2-N9	1.415	N1-N9	1.394	C4-N9	1.362	C4-N9	1.357	N1-N9	1.395	N2-N9	1.389
N9-H10	1.019	N9-H10	1.020	N9-H10	1.013	N9-H10	1.012	N9-H10	1.017	N9-H10	1.022
N9-H11	1.015	N9-H11	1.017	N9-H11	1.012	N9-H11	1.011	N9-H11	1.021	N9-H11	1.015
C3-H12	1.082	C3-H12	1.080	N2-H12	1.026	N1-H12	1.019	C4-H12	1.082	C4-H12	1.083
C5-O13	1.193	C5-O13	1.199	C5-O13	1.209	C5-O13	1.215	C5-O13	1.219	C5-O13	1.208
N1-N2-C3	104.4	N1-N2-C3	108.2	O7-O13	2.820	N1-N2-N3	107.1	O7-O8	2.777	O7-O13	2.820
N2-C3-N4	112.9	N2-C3-N4	109.8	N1-N2-N3	102.9	N2-N3-C4	108.3	N1-N2-N3	103.8	N1-N2-C3	103.6
C3-N4-C5	107.8	C3-N4-C5	108.2	N2-N3-C4	111.4	N3-C4-C5	110.1	N2-N3-C4	111.2	N2-C3-C4	110.5
N4-C5-N1	103.6	N4-C5-N1	104.7	N3-C4-C5	109.8	C4-C5-N1	104.9	C3-C4-C5	108.8	C3-C4-C5	110.1
C5-N1-N2	110.6	C5-N1-N2	107.9	C4-C5-N1	102.8	C5-N1-N2	109.1	C4-C5-N1	103.6	C4-C5-N1	104.5
H10-N9-H11	111.2	H10-N9-H11	109.1	C5-N1-N2	111.7	H10-N9-H11	117.5	C5-N1-N2	111.7	C5-N1-N2	109.5
N1-N6-O7	113.5	N2-N6-O7	112.6	H10-N9-H11	116.6	N2-N6-O7	112.4	H10-N9-H11	107.8	H10-N9-H11	110.2
O7-N6-N1-N2	−174.9	O7-N6-N2-N1	−158.8	N1-N6-O7	113.2	O7-N6-N2-N1	21.01	N2-N6-O7	111.9	N1-N6-O7	113.1
H10-N9-N2-N1	−99.9	H10-N9-N1-N2	−119.8	O7-N6-N1-N2	1.2	H10-N9-C4-N3	−18.4	O7-N6-N2-N1	179.2	O7-N6-N1-N2	−177.2
C3-N4-C5-O13	−174.8	C3-N4-C5-O13	−171.7	H10-N9-C4-N3	−18.5	H12-N1-C5-O13	−38.5	H10-N9-N1-C5	−81.8	H10-N9-N2-N3	39.1
O8-N4-C3-N2	−173.9	O8-N4-C3-N2	−178.3	H12-N2-N3-O8	56.2	O8-N3-N2-N1	−175.4	H12-C4-C5-O13	3.0	H12-C4-C5-O13	4.0
				O8-N3-N2-N1	173.6			O8-N3-C4-C5	−179.7	O8-N3-C4-C5	−173.9

[a] Bond lengths in Å and angles in deg

reaction ($\Delta_r H_{298K}$), i.e., the bond dissociation enthalpy (DH$_{298K}$) of the molecule (A-B)

$$A-B(g) \rightarrow A^{\cdot}(g) + B^{\cdot}(g) \qquad (7)$$
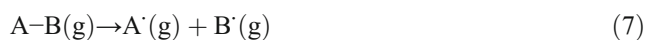
It is the reaction enthalpy of the bond homolysis and hence depends on the enthalpies formation of reactants and products.

$$\Delta_r H_{298K} = \Delta_f H_{298.K}(A^{\cdot})$$
$$+ \Delta_f H_{298K}(B^{\cdot}) - \Delta_f H_{298K}(A-B)$$
$$= DH_{298K}(A-B) \qquad (8)$$

where $\Delta_f H_{298K}(A^{\cdot})$ and $\Delta_f H_{298K}(B^{\cdot})$ are the enthalpies of formation of radicals and $\Delta_f H_{298\ K}(A-B)$ is the enthalpy of formation of the molecule.

However at 0 K the homolytic bond dissociation energy can be given as

$$BDE_0(A-B) = E_0(A^{\cdot}) + E_0(B^{\cdot}) - E_0(A-B) \qquad (9)$$

The bond dissociation energy with ZPE correction may be written as

$$BDE(A-B)_{ZPE} = BDE_0(A-B) + \Delta ZPE \qquad (10)$$

Atoms-in-molecule (AIM) [19] analyses of the optimized geometries of title compounds have also been carried out to check the presence of intramolecular interactions and the strength of bonds. We have searched for the (3,-1) bond critical points that could be associated with an intramolecular interactions and the bonds and then examined for the properties: the electron density $\rho(r_c)$, Laplacian of charge density $\nabla^2\rho(r_c)$ (defined as the sum of the hessian eigenvalues) and the ratio of the eigenvalues $|\lambda_1|/\lambda_3$. The sum of the three hessians (λ_1, λ_2, λ_3) at a bond critical point, the quantity $\nabla^2\rho$, provide the useful characterization of the manner in which the electronic charge density is distributed in the internuclear region. If the value of charge density ρ ($> 10^{-1}$ a.u.) and the curvature are large, Laplacian of charge density may be positive or negative usually in the same order of magnitude as ρ then the interaction is of shared type typical of covalent interaction. For the closed-shell interactions, such as hydrogen bond interactions, van der Waals interactions and ionic systems, the charge density ρ ($\approx 10^{-2}$ to$\approx 10^{-3}$ a.u.) at the bond critical point is quite small and the Laplacian of the charge density is positive.

Results and discussion

Optimized structures

We have optimized the structures of triazolone-N-oxide molecules at the B3LYP/aug-cc-pVDZ level and their optimized structures are as shown in Fig. 1. The selected structural parameters of model molecules optimized at the B3LYP/aug-cc-pVDZ level are listed in Table 1. The lowest frequency, total energy, zero-point energy, thermal correction to enthalpy and frontier molecular orbital energies and their gaps and heats of formation of triazolone-N-oxides are presented in Table 2. All the model compounds belong to C_1 point group with non-planarity. The N→O lengths of the optimized structures indicates that N→O bond is longer in molecules 6 (1.297 Å), 5 (1.288 Å), 1 (1. 277 Å), 2 (1.274 Å), 7 (1. 262 Å), 8 (1.258 Å), 9 (1. 254 Å), 4 (1.253 Å) and 10 (1. 251 Å). However, the N→O length is shorter in 11 (1.242 Å), 12 (1.232 Å) and 3 (1.236 Å). As seen from Table 1, the increasing order of N-NO bond length is 5<6<9<10<8~3<2<4<7<1<12< 11. The C=O distances vary from 1.193 to 1.220 Å and the N-N=O angles vary from 113 to 115.5^0. The nitrogen atom (N6) of the N=O group in compounds 2, 3, 5, 6, 8 and 9 molecule forms almost in-plane with the 5-membered triazole ring plane. However, in compounds 1, 4, 7, 10 and 12, the nitrogen atom of the N=O group deviates at about ± 33–41^0 from the 5-membered ring plane. Interestingly, the nitrogen atom of the NO group deviates significantly at about ± 80^0 from the ring plane in 11. The nitrogen atom (N9) of the NH$_2$ group in molecules 1, 2, 4, 5, 6, 9 and 10 molecule forms almost in-plane with the ring plane. However, in compounds 3, 7, 8, 11 and 12, the nitrogen atom of the NH$_2$ group deviates at about ± 29–57^0 from the ring plane. The interatomic distances of O-O in compounds 11 and 12 are 2.777 (O7-O8) and 2.820 (07-O13) Å, respectively. To check the presence of intramolecular interactions in the molecules, atoms-in-molecule (AIM) theory of Bader [19] has been applied to the molecules. Using the optimized structures computed from the B3LYP/aug-cc-pVDZ level, we have searched for the (3,-1) bond critical points. AIM analysis of molecules 11 and 12 have clearly shown that the (3,−1) bond critical point in between O-O and thus confirm the existence of O…O interaction. As seen from Table 2S, the Laplacian of charge density $\nabla^2\rho$ is positive and the small value of ρ at the intramolecular (3,−1) bond critical points have been indicated as the closed-shell type interaction.

Frontier molecular orbitals

The highest occupied molecular orbitals (HOMO) and the lowest unoccupied molecular orbitals (LUMO) play a vital role in governing the chemical reactions of the compounds [17]. The band gap ($\Delta E_{(LUMO-HOMO)}$) between the LUMO and HOMO is an important stability index of the molecules. A large band gap implies high stability and small band gap implies low stability, i.e., the smaller the band gap between HOMO and LUMO, the easier the electron transition and the lower the stability of the explosive will be. In all the molecules, the HOMO is found to be spread over the entire molecule, but the LUMO is localized over the oxygen atoms. The frontier molecular orbital energies and their differences are presented in Table 2. The designed compounds **12** (0.15518 a.u.) and **3** (0.13457 a.u.) are more stable while the title compounds **1** (0.10913 a.u.) and **2** (0.10535 a.u.) are less stable. The high frontier orbital gap is also associated with a low chemical reactivity and high kinetic stability [20, 21]. Thus the designed compound **12** seems to be kinetically more stable and chemically less active than the other triazolone-N-oxides. The discrepancies in the band gap values among the isomers are caused by the relative positions of N=O, NH_2, N→O and C=O groups in the triazole ring.

AIM analysis

The electron density analysis on the bond of triazolone-N-oxide compounds has been carried out to understand the bond strength. The electron density from the AIM theory is relatively independent of basis set and induction of electron correlation compared to other methods such as Mulliken population analysis and its variations [19]. The weakest bond in the molecule is believed to be the initial step in the decomposition or detonation. Hence, the property of bond is used to show the relationship with the impact sensitivity of compounds [1, 3]. Table 3 give the electron density of the bond critical point corresponding to the X-Y (where, X=C or N) bonds of designed molecules. As seen from Table 3, the Laplacian of charge density $\nabla^2 \rho$ is negative and the larger value of ρ at the (3,-1) bond critical points indicate the shared type of covalent interaction. The greater the electron density of X-Y bond the higher the bond strength, which in turn is expected to lower the impact sensitivity. From the electron density values, it can be attributed that the weakest bond is found to be in the ring for triazolone-N-oxides with the exception of **11**. This is due to the presence of adjacent N→O and an amino group increases the non-planarity of N=O group, which weakens the N-NO bond.

Bond dissociation energies

Studies of the bond dissociation energies (BDE) provide useful information about the stability of model compounds. The stability/or sensitivity of compound depends on temperature, nature of materials and explosophores in the molecular structure. A systematic study of this quantity should be useful in understanding initiation events. The initial stages in the

Table 2 Lowest frequency (ω_L), total energy (E_o), zero-point energy (ZPE), thermal correction to enthalpy (H_T), frontier orbital energies and heats of formation (HOF) of triazolone-N-oxides computed at the B3LYP/aug-cc-pVDZ level

Entry	ω_L (cm^{-1})	E_0 (a.u.)	ZPE (a.u.)	H_T (a.u.)	HOMO (a.u)	LUMO (a.u.)	$\varepsilon_{(LUMO-HOMO)}$ (a.u.)	HOF (kJ mol^{-1})
1	39	−577.3602493	49.30001	0.088981	−0.21857	−0.10944	0.10913	74.32
2	84	−577.3667584	49.75889	0.089430	−0.22679	−0.12144	0.10535	78.41
3	82	−577.3303198	50.13519	0.089692	−0.25672	−0.12215	0.13457	114.77
4	55	−577.3162307	49.48780	0.089143	−0.23875	−0.12093	0.11782	150.32
5	67	−577.3682166	50.16163	0.089867	−0.23375	−0.12304	0.11071	75.74
6	54	−577.3623101	50.23928	0.089803	−0.22968	−0.11895	0.11073	150.32
7	74	−577.2977522	49.50271	0.088762	−0.24654	−0.12791	0.11862	197.84
8	86	−577.3115353	50.09872	0.089620	−0.25479	−0.13058	0.12421	163.90
9	42	−577.342185	50.29285	0.089973	−0.25232	−0.12633	0.12599	84.36
10	73	−577.3401477	49.79063	0.089219	−0.24787	−0.12126	0.12661	69.55
11	65	−577.291978	49.26331	0.088839	−0.26130	−0.15086	0.11044	114.80
12	68	−577.2964814	49.39920	0.088564	−0.27362	−0.11844	0.15518	102.25
1,2,3-Triazole	592	−242.2616263	36.94842	0.063414	−0.27746	−0.02324	0.25422	271.7[a]
1,2,4-Triazole	573	−242.287813	37.45686	0.064187	−0.28409	−0.01989	0.26420	192.7[a]
CH_4	1304	−40.5206269	27.75552	0.048050	−0.39345	−0.00693	0.38652	−74.6[a]
CH_3NH_2	149	−95.8668603	38.76368	0.066397	−0.21836	−0.01000	0.20836	−22.5[a]
CH_3ONO_2	15	−320.2336644	33.40970	0.058612	−0.31093	−0.09814	0.21279	124.4[a]

[a] from ref [12]

Table 3 Properties of (3, -1) bond critical point in model compounds computed at the B3LYP/aug-cc-pVDZ level

Table 3 (continued)

Molecule	Bond	r (Å)	$\rho(r_C)$ (eÅ^{-3})	$\nabla^2\rho(r_C)$ (eÅ^{-5})
1	N1-N6	1.426	2.10	−11.4
	N1-N2	1.457	1.98	−11.5
	N2-C3	1.316	2.38	−21.4
	C3-N4	1.384	2.09	−23.2
	N4-C5	1.394	2.05	−22.0
	C5-N1	1.425	1.95	−19.2
	C3-N9	1.367	2.20	−25.2
2	N1-N2	1.427	2.13	−14.4
	N2-C3	1.312	2.38	−18.8
	C3-N4	1.393	2.06	−22.5
	N4-C5	1.448	1.83	−16.2
	C5-N1	1.387	2.10	−23.0
	N4-N6	1.399	2.24	−13.7
	C3-N9	1.363	2.21	−25.3
3	N1-N2	1.468	1.97	−11.5
	N2-C3	1.316	2.28	−9.8
	C3-N4	1.395	2.00	−20.4
	N4-C5	1.420	1.96	−19.6
	C5-N1	1.392	2.08	−22.2
	N1-N9	1.365	2.36	−16.6
	N4-N6	1.382	2.34	−15.3
4	N1-N2	1.448	2.05	−12.9
	N2-C3	1.314	2.31	−12.1
	C3-N4	1.389	2.05	−22.2
	N4-C5	1.387	2.10	−22.5
	C5-N1	1.430	1.90	−17.7
	N4-N9	1.395	2.21	−15.3
	N1-N6	1.437	2.07	−11.2
5	N1-N2	1.396	2.24	−15.6
	N2-C3	1.378	2.10	−23.1
	C3-N4	1.332	2.39	−29.5
	N4-C5	1.450	1.89	−17.0
	C5-N1	1.412	1.99	−20.3
	C3-N9	1.338	2.31	−28.5
	N2-N6	1.345	2.51	−16.9
6	N1-N2	1.408	2.20	−48.6
	N1-C5	1.437	1.85	−16.9
	C5-N4	1.426	1.98	−43.2
	N4-C3	1.335	2.38	−34.2
	C3-N2	1.387	2.12	−23.9
	C3-N9	1.337	2.31	−28.9
	N1-N6	1.347	2.52	−17.4
7	N1-N2	1.417	1.99	−19.9
	N2-C3	1.398	2.06	−22.3
	C3-N4	1.319	2.35	−19.3
	N4-C5	1.488	1.77	−14.0
	C5-N1	1.407	2.00	−10.5
	N1-N6	1.453	2.18	−49.0

Molecule	Bond	r (Å)	$\rho(r_C)$ (eÅ^{-3})	$\nabla^2\rho(r_C)$ (eÅ^{-5})
	N2-N9	1.415	2.15	−14.6
8	N1-N2	1.405	2.23	−15.8
	N2-C3	1.379	2.06	−20.9
	C3-N4	1.327	2.32	−20.3
	N4-C5	1.482	1.79	−14.7
	C5-N1	1.389	2.09	−22.5
	N2-N6	1.382	2.33	−14.8
	N1-N9	1.394	2.22	−15.2
9	N1-N2	1.411	2.20	−15.2
	N2-N3	1.439	2.11	−14.2
	N3-C4	1.325	2.27	−14.3
	C4-C5	1.455	1.92	−16.3
	C5-N1	1.431	1.86	−17.2
	N1-N6	1.354	2.48	−16.9
	N2-N9	1.361	2.19	−25.5
10	N1-N2	1.395	2.26	−15.8
	N2-N3	1.449	2.05	−15.9
	N3-C4	1.324	2.27	−14.2
	C4-C5	1.463	1.89	−15.9
	C5-N1	1.406	1.99	−20.3
	N2-N6	1.379	2.37	−15.2
	C4-N9	1.357	2.21	−26.1
11	N1-N2	1.384	2.36	−17.1
	N2-N3	1.432	2.15	−14.0
	N3-C4	1.332	2.17	−7.1
	C4-C5	1.447	1.93	−16.1
	C5-N1	1.415	1.95	−19.1
	N2-N9	1.395	2.23	−15.4
	N1-N6	1.761	1.02	−1.8
12	N1-N2	1.417	2.21	−15.7
	N2-N3	1.476	1.96	−11.4
	N3-C4	1.319	2.22	−5.0
	C4-C5	1.451	1.91	−16.0
	C5-N1	1.448	1.81	−15.6
	N1-N6	1.466	1.96	−10.0
	N2-N9	1.390	2.28	−51.3

decompositions of energetic materials can be assumed on the basis of the BDEs. In general, the larger the BDE value of the N-NO bond breaking, the higher the stability will be. Hence, the calculated BDE for removal of the NO group can be used to index the relative strength of the compounds. Conversely this is only applied to the molecules in which the N−NO bond is the weakest. The nitroso group often represents the primary cause of initiation reactivity of model compounds. We have computed N-NO, C=O, N→O bonds at the UB3LYP/aug-cc-pVDZ level. The bond dissociation energies of triazolones are

shown in Table 4. The designed compounds (3 and 4) have N-NO bond dissociation energy values 54.71, 46.78 kcal mol^{-1} respectively higher compared to RDX (39.2 kcal mol^{-1}). These values in case of other isomers the bond dissociation energies are lower compared to RDX. The calculated BDE values of C=O and N→O bonds are higher compared to the experimental values [1, 3]. The position of N=O, N→O and C=O group in the structure has strong influence on the BDE value. It is worthy of note that the adjacent groups BDE is less for the pyrolysis. The compound could be considered as a practical energetic material if it has BDEs more than ~20.07 kcal mol^{-1} [3]. However, this is only marginally sufficient to make the compound metastable and it would have preferable stability if BDE>30.11 kcal mol^{-1}. Also, it can be deduced that the designed compounds 1, 2, 4, 5, 6, 8 and 9 have no sufficient energy barrier against the removal of N=O, and thus are not stable enough for practical use.

Heat of formation

Isodesmic reactions were implemented to achieve better accuracy for the gas phase heats of formation of model compounds. These are hypothetical reactions that incorporate similar bonding environments for both reactants and products, which allow for cancellation of error associated with method of analysis [22]. The heats of formation (HOF) of triazol-5-one-N-oxides with the reference compounds are shown in Table 2. The model compound 7 showed higher heat of formation (197.84 kJ mol^{-1}) however, the compound 10 showed lower heat of formation

(69.55 kJ mol^{-1}). The compounds 4 and 6 showed equal heats of formation (150.32 kJ mol^{-1}). The total heats of formation depend upon the relative proportions of the reactants to the products. The heats of formation values are related to the relative positions of substituent groups and the strength of C-C, C-N, N-N, N-O, C-O bonds. The calculated heats of formation values do not exactly agree with those obtained experimentally because the conditions of loading density, temperature, pressure and so on are not taken into consideration [1, 3, 11].

Crystal density

Density appears to a higher power in the Kamlet-Jacob equations than does any variables. The detonation velocity linearly increases with ρ for most explosives. The detonation pressure increases with the square of ρ, when ρ is greater than one. Many researchers have attempted to predict the densities with satisfactory accuracy [23–25]. We have taken the optimized structures computed from the B3LYP/aug-cc-pVDZ level to predict the crystal density using Materials Studio 4.1 package with various force fields. Several organic compounds are known to pack in P2$_1$, P2$_1$/c, P2$_1$2$_1$2$_1$, P-1, Pbca, Pbcn, Pna2$_1$, C2/c, C$_C$ and/or C$_2$ space groups [26]. The densities of RDX, HMX, ONC and CL-20 computed from the B3LYP/aug-cc-pVDZ level are 1.817, 1.910, 2.054 and 2.075 g/cm^3 that are comparable with the experimental values 1.82, 1.92, 1.979 and 2.042 g/cm^3, respectively [27–29]. We carefully compared the densities predicted from various force fields and found that the calculated values obtained using cvff force field were found to be higher. The predicted crystal structures of selected triazol-5-one-N-oxides using cvff force field are shown in Fig. 2. The values obtained from compass, compass26 and compass27 are lower compared with the values obtained from dreiding force field. However, the calculated values obtained using Eq. (3) were found to be lower compared to the values obtained from cvff force field. The calculated densities using various force fields and as per Eq. (3) are shown in Table 5. The model compounds have densities varying from 1.943 to 1.956 g/cm^3. The absolute error in the calculated crystal densities according to ref [14] are expected to be reliable to estimate the detonation properties.
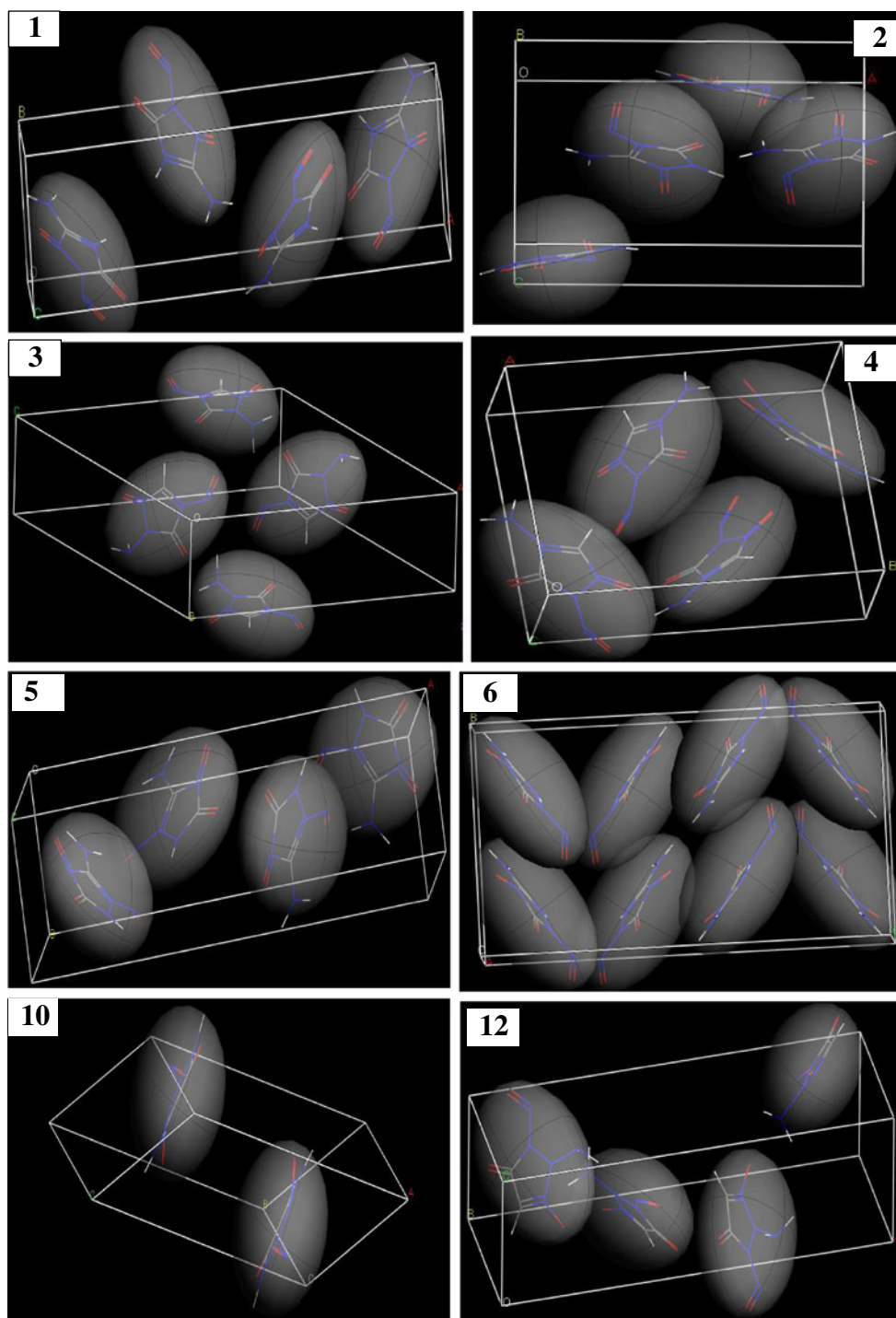
Performance properties

Detonation velocity (D) and detonation pressure (P) are important factors to evaluate the performance of explosives. Based on the heat of formation, predicted crystal density,

Table 4 Bond dissociation energies (BDEs) of model compounds computed from UB3LYP/aug-cc-pVDZ level

Molecule	BDE$_{N-NO}$ (kcal mol^{-1})	BDE$_{N-O}$ (kcal mol^{-1})	BDE$_{C-O}$ (kcal mol^{-1})	ε (LUMO-HOMO) (a.u.)
1	16.164	36.142	164.242	0.10913
2	14.472	33.154	183.351	0.10535
3	54.715	33.212	164.605	0.13457
4	46.782	35.602	163.532	0.11782
5	14.235	35.205	174.345	0.11071
6	12.448	33.412	172.208	0.11073
7	35.121	34.104	161.361	0.11862
8	18.664	37.407	173.704	0.12421
9	15.556	34.643	174.736	0.12599
10	28.965	37.703	165.645	0.12661
11	26.852	35.741	165.652	0.11044
12	26.852	35.603	164.702	0.15518

number of decomposition products and average molecular weight of decomposition products, we have calculated the detonation velocity and detonation pressure using Kamlet-Jacob equations. The calculated D and P of CL-20, ONC, RDX and HMX computed from the B3LYP/aug-cc-pVDZ level are 9.34, 10.06, 8.86, 9.10 km/s and 43.10, 50.0, 34.23, 39.40 GPa respectively. For CL-20, ONC, RDX and HMX, the experimental D and P are 9.20, 10.10,

Table 5 Calculated densities of triazolone-N-oxides

Entry	Dreiding	Universal	Compass	Compass26	Compass27	cvff	Politzer's approach [14]
1	1.745	1.686	1.457	1.441	1.457	2.133	1.956
2	1.761	1.693	1.441	1.422	1.383	2.128	1.951
3	1.737	1.657	1.472	1.477	1.471	2.122	1.944
4	1.716	1.668	1.434	1.397	1.437	2.111	1.947
5	1.653	1.682	1.472	1.471	1.471	2.098	1.952
6	1.763	1.586	1.423	1.428	1.428	2.111	1.943
7	1.731	1.668	1.427	1.441	1.465	2.134	1.948
8	1.698	1.583	1.468	1.424	1.511	2.132	1.946
9	1.695	1.584	1.484	1.432	1.576	2.114	1.952
10	1.761	1.617	1.411	1.421	1.411	2.147	1.954
11	1.743	1.611	1.438	1.357	1.402	2.133	1.955
12	1.741	1.663	1.442	1.412	1.402	2.132	1.957

8.75, 8.96 km/s and 42.0, 48.45, 34.70, 35.96 GPa respectively [26–28]. The densities calculated as per the procedure of Politzer's approach has been used for the determination of detonation velocity and detonation pressure. The explosive properties of triazolone-N-oxides are summarized in Table 6. The calculated detonation velocity and pressure of **4** (D 10.0 km/s and P 46.55 GPa), **6** (D 10.0 km/s and P 46.36 GPa), **7** (D 10.46 km/s and P 50.87 GPa) and **8** (D 10.14 km/s and P 47.76 GPa) are comparable with those of CL-20 and ONC. An exceptionally higher performance of compound **7** is presumably due to its higher heat of formation (197.84 kJ mol^{-1}) and density (1.948 g/cm^3).

Conclusions

The molecular orbital calculations at the B3LYP/aug-cc-pVDZ level were performed to explore the electronic structure, stability, electron density, heat of formation, detonation velocity and detonation pressure of triazolone-N-oxides. The band gap values of model molecules vary from 0.10535 to 0.15518 a.u. The model compound **12** seems to be kinetically more stable and chemically less active than the other triazolone-N-oxides. Heats of formation of triazolone-N-oxides have been computed at the same level of theory via isodesmic reaction procedure. Kamlet-Jacob equations were used to calculate the detonation

Table 6 Explosive properties of triazolone-N-oxides and reference compounds

Entry	Formula	Mw (g mol^{-1})	OB%	Q (kcal g^{-1})	ρ (g cm^{-3})	D (km s^{-1})	P (GPa)
1	$C_2H_3N_5O_3$	145	−27.58	1.148	1.956	9.17	39.13
2	$C_2H_3N_5O_3$	145	−27.58	1.212	1.951	9.20	39.37
3	$C_2H_3N_5O_3$	145	−27.58	1.463	1.944	9.62	42.94
4	$C_2H_3N_5O_3$	145	−27.58	1.708	1.947	10.02	46.55
5	$C_2H_3N_5O_3$	145	−27.58	1.193	1.952	9.17	39.11
6	$C_2H_3N_5O_3$	145	−27.58	1.708	1.943	10.0	46.36
7	$C_2H_3N_5O_3$	145	−27.58	2.036	1.948	10.46	50.87
8	$C_2H_3N_5O_3$	145	−27.58	1.801	1.946	10.14	47.76
9	$C_2H_3N_5O_3$	145	−27.58	1.253	1.952	9.26	40.07
10	$C_2H_3N_5O_3$	145	−27.58	1.151	1.954	9.12	38.50
11	$C_2H_3N_5O_3$	145	−27.58	1.464	1.955	9.66	43.44
12	$C_2H_3N_5O_3$	145	−27.58	1.376	1.957	9.52	42.22
TNT[a]	$C_7H_5N_3O_6$	227	−74.0	0.88	1.654	6.90	22.30
RDX[a]	$C_3H_6N_6O_6$	222	−21.62	1.27	1.82	8.75	34.70
HMX[a]	$C_4H_8N_8O_8$	296	−21.62	1.27	1.92	8.96	35.96
NTO[b]	$C_2H_2N_4O_3$	130	−24.60	1.03	1.918	8.56	31.12
CL-20[c]	$C_3H_6N_{12}O_{12}$	438	−11.0	1.342	2.042	9.20	42.0
ONC[d]	$C_8N_8O_{16}$	464	0	1.337	1.979	10.10	48.45

[a] Experimental values of 2,4,6-trinitrotoluene (TNT), 1,3,5-trinitroperhydro-1,3,5-triazine (RDX) and octahydro-1,3,5,7-tetrnitro-1,3,5,7-tetrazocine (HMX) are from ref [26]

[b] Experimental values of 3-nitro-l,2,4-triazol-5-one (NTO) are from ref [2]

[c] Experimental values of 2,4,6,8,10,12-Hexanitro-2,4,6,8,10,12-hexaazaisowurtzitane (CL-20) are from ref [27]

[d] Experimental values of octanitrocubane (ONC) are from ref [28]

velocity and detonation pressure. The designed compounds **4**, **6**, **7** and **8** have shown higher performance compared with those of 2,4,6,8,10,12-hexanitro-2,4,6,8,10,12-hexaazaisowurtzitane and octanitrocubane. Atoms-in-molecule (AIM) analyses have also been carried out to understand the nature of intramolecular interactions in the designed molecules. The NO, NH_2 group, C=O and N-oxide groups increases the heat of explosion, density, detonation velocity and detonation pressure tremendously. The model compounds satisfy the criteria as the high energy materials.

References

1. Larina L, Lopyrev V (2009) Nitroazoles-Synthesis, Structure and Application. Springer, New York
2. Lee KY, Coburn MD (1985) 3-Nitro-1,2,4-triazol-5-one, a less sensitive explosive, LA10302 MS. Los Alamos National Laboratory, Los Alamos
3. Klapotke TM (2007) High energy density materials. Springer, Berlin
4. Frisch MJ, Trucks GW, Schlegel HB, Scuseria GE, Robb MA, Cheeseman JR, Montgomery JA, Vreven T, Kudin KN, Burant JC, Millam JM, Iyengar SS, Tomasi J, Barone V, Mennucci B, Cossi M, Scalmani G, Rega N, Petersson GA, Nakatsuji H, Hada M, Ehara M, Toyota K, Fukuda R, Hasegawa J, Ishida M, Nakajima T, Honda Y, Kitao O, Nakai H, Klene M, Li X, Knox JE, Hratchian HP, Cross JB, Adamo C, Jaramillo J, Gomperts R, Stratmann RE, Yazyev O, Austin AJ, Cammi R, Pomelli C, Ochterski JW, Ayala PY, Morokuma K, Voth GA, Salvador P, Dannenberg JJ, Zakrzewski VG, Dapprich S, Daniels AD, Strain MC, Farkas O, Malick DK, Rabuck AD, Raghavachari K, Foresman JB, Ortiz JV, Cui Q, Baboul AG, Clifford S, Cioslowski J, Stefanov BB, Liu G, Liashenko A, Piskorz P, Komaromi I, Martin RL, Fox DJ, Keith T, Al-Laham MA, Peng CY, Nanayakkara A, Challacombe M, Gill PMW, Johnson B, Chen W, Wong MW, Gonzalez C, Pople JA (2003) Gaussian 03, Revision B.04. Gaussian, Inc, Pittsburgh, PA
5. Kohn W, Sham LJ (1965) Phys Rev 140:A1133
6. Parr RG, Yang W (1989) Density Functional Theory of Atoms and Molecules. Oxford University Press, London
7. Becke AD (1988) Phys Rev A 38:3098
8. Vosko SH, Vilk L, Nusair M (1980) Can J Phys 58:1200
9. Lee C, Yang W, Parr RG (1988) Phys Rev B 37:785
10. Hehre WJ, Ditchfield R, Radom L, Pople JA (1970) J Am Chem Soc 92:4796
11. Ravi P, Venkatesan V, Tewari SP, Sikder AK (2010) J Hazard Mate 183:859
12. Lide, D.R. CRC Hand Book of Chemsitry and Physics, 84th Ed., CRC Press, 2003–2004.
13. Materials Studio 4.1, Accelrys Inc, San Diego, CA, 2004.
14. Politzer P, Martinez J, Murray JS, Concha MC, Toro-Labbe A (2009) Mol Phys 107:2095
15. Kamlet MJ, Jacobs SJ (1968) J Chem Phys 48:23
16. Akhavan J (1998) Chemistry of explosives. The Royal Society of Chemistry, Cambridge
17. Fukui F, Yonezawa T, Shingu H (1952) J Chem Phys 20:722
18. Zhou Z, Parr RG (1990) J Am Chem Soc 112:5720
19. Bader RFW (1994) Atoms in molecules. Clarendon, Oxford
20. Hess BA Jr, Schaad LJ (1971) J Am Chem Soc 93:2413
21. Murray JS, Sen KD (1996) Molecular electrostatic potentials: concepts and applications. Elsevier, Amsterdam
22. Hehre WJ, Ditchfield R, Radom L, Pople JA (1970) J Am Chem Soc 92:4796
23. Cho SG, Goh EM, Kim JK (2001) Bull Korean Chem Soc 22:775
24. Kim CK, Cho SG, Kim CK, Park HY, Zhang H, Lee HW (2008) J Comput Chem 29:1818
25. Belsky VK, Zorkii PM (1977) Acta Cryst A 13:1004
26. Mathieu J, Stucki H (2004) Chimia 58:383
27. Hoffman DM (2003) Prop Explos Pyrotech 28:194
28. Eaton PE, Gilardi R, Zhang MX (2000) Adv Mat 12:1143